MODELING OF TEXAS GULF COAST GEOPRESSURED GEOTHERMAL AQUIFERS

R. M. Knapp, M. H. Dorfman and O. F. Isokrari*
Petroleum Engineering Department
The University of Texas at Austin
Austin, Texas 78712

We would like to report that, at this time, we have coded and tested a model that simulates the behavior of a geopressured geothermal aquifer as it is subjected to production from one or more wells. We have tested this simulator by checking its computed responses against results reported for systems that span the range of the abilities of the simulator.

The general objective of our work was to develop and test a simulator for geopressured geothermal aquifers. The simulator considers the effects of heterogeneous and anisotropic porous media, and the presence of two fluid phases, water and natural gas. The natural gas can exist either in solution or as a separate and distinct flowing phase. The model includes several drive mechanisms which we feel will be significant: these include the water compressibility, the rock matrix compressibility, the changes that occur in pore volume as the aquifer is compacted, the influx of water from adjacent shales either at the edge of the sandstone body or immediately above it or below it, and the expansion of the natural gas either in solution or as a free-phase. We feel that such a model can be used for depletion studies. With the addition of thermal effects it can be used to study the feasibility of reinjection of "cool" used water.

The simulator is the result of combining the momentum transport equation for water and gas with constitutive equations describing the changes of fluid properties with pressure and the changes of formation parameters, such as porosity, permeability and formation thickness with decreasing pore pressure. The resulting equations, shown in the appendix, are solved using finite difference methods to obtain pressure distributions within the aquifer. The energy transport equation can be added to the set of equations and solved to obtain temperature distributions. At the University of Texas, we have done this in a decoupled fashion in order to examine long-term effects. We do not feel that this is adequate for the thermodynamically demanding case of water reinjection.

The goal of the model development was to have a mechanism for performing reservoir engineering studies on potential geopressured geothermal aquifers. The first example of this was performed on a prospect in eastern Kenedy County, Texas, (Knapp and Isokrari, 1976). An isopachous map of the prospect was used to construct a rectangular cube of equal volume and area. This resulted in a reservoir 4.5 miles by 9 miles that was 162 feet thick. At the expected initial pressure of 11,000 psia, the average formation porosity was estimated to be 0.216 and the average permeability was estimated to be

---

*Dr. Isokrari is now with Amoco Production Company, P. O. Box 591, Tulsa, Oklahoma 74102.

18 millidarcies based on well log and core data. The reservoir fluid was assumed to be fresh water at 300°F. Five depletion studies using a single well producing 40,000 BBLS/day were made to investigate the effectiveness of various drive mechanisms. These are shown in Fig. 1. In the first case, the only active producing mechanism was the expansion of the water. It will be noted that the producing well pressure drops to 5,000 psi in about 7 years. We stopped the calculations at that point because 5,000 psi is approximately the hydrostatic pressure at the expected well depth of 13,000 feet. For Case II, a rock matrix compressibility of 7.5×10^{-6} psi^{-1} was added. It can be seen that the well pressure dropped to just below 8,000 psia after 30 years of production. A compaction coefficient of 4.6×10^{-6} psi^{-1} was added for Case III. In this instance, the well pressure remains above 9,000 psia for the full thirty-year producing period. To simulate the effects of shale water influx from off-shore shales, a shale section was added which has a width of 2.5 miles and a length and thickness identical to that of the sandstone formation. The shale porosity at 11,000 psia was assumed to be the same as the sandstone porosity, or 0.216; the initial shale permeability was estimated to be 10^{-4} millidarcies and the shale matrix compressibility was assumed to be 7.5×10^{-4} psi^{-1}. The shale uniaxial compaction coefficient was assumed to be 4.6×10^{-5} psi^{-1}. This run is shown as Case IV. The well block pressure is sustained at a higher level than in the other runs although the amount of support due to shale water influx is not greatly enhanced. Other runs, on a reduced system, show that the effects of underlying sediments are much greater (Knapp and Isokrari, 1976). Finally, the effects of adding 44.1 scf/STB of natural gas to the formation water are shown as Case V in Fig. 1. The small amount of gas along with its very small saturation combine to provide only a small amount of additional pressure support for production.

Since one well would not produce enough water for significant electric power production, the depletion of the aquifer using eleven 40,000 BBLS/day wells was simulated. The average reservoir pressure fell below 7,000 psi in about ten years. The single sand unit could not support a power generation plant for a long enough period of time to depreciate it. There are, however, other sand bodies of a similar size in this prospect that could also be produced, which would extend the useful life of the system.

The model was next used to study the production of natural gas from geopressured geothermal aquifers, (Isokrari and Knapp, 1976). We classified such aquifers into three types based on the natural gas content. In Type 1, the reservoir water is undersaturated with natural gas. However, it could still contain more than 40 standard cubic feet of natural gas per reservoir barrel of water at reservoir conditions. In Type 2 reservoirs, the reservoir water is fully saturated with natural gas and the reservoir may contain a small gas cap. Type 3 is a geopressured gas reservoir. The water is nearly immobile in the reservoir but the adjacent and underlying shales contain water with gas in solution, that may move into the reservoir.

Computer runs were made to generate a variety of data. For Type 1 and Type 2 reservoirs, reservoir pressure variations with natural gas and water production were generated. It was found that substantial amounts of natural gas can be produced over a long period of time.

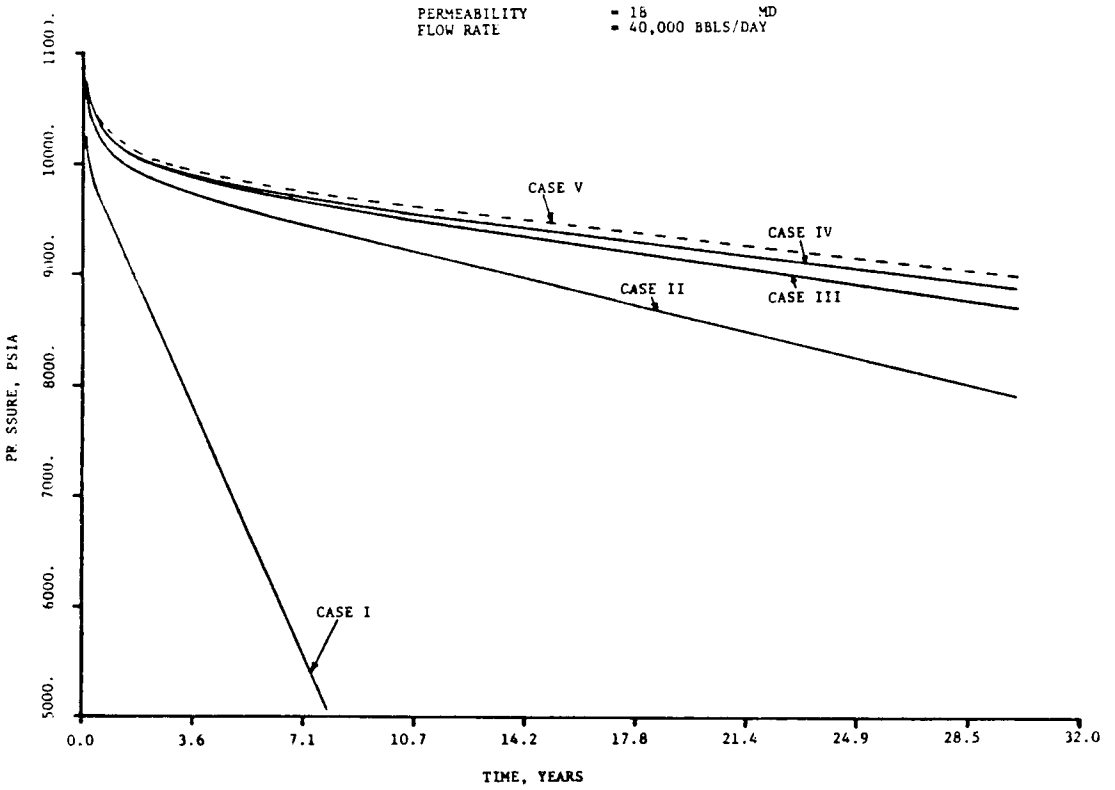

Figure 1

PRESSURE WELL BLOCK PORE PRESSURE OF VARIOUS RESERVOIR DRIVES WITH TIME

The model was used to make areal studies of a bounded hypothetical geopressured gas reservoir, with no shale water influx using different compaction coefficients. It was found the P/Z (average reservoir pressure divided by gas deviation factor) versus cumulative production curve changes significantly with an increase in compaction coefficients.

The model was also used to make cross-sectional studies to assess the effects of shale water influx from adjacent and underlying shales.

Finally, the model was used to simulate the reported production history of the Anderson 'L' zone, a geopressured Frio (Oligocene) gas reservoir in South Texas described by Duggan (1972). Good agreement was obtained between the observed and calculated pressures and water production versus cumulative gas production.

References

Duggan, J. L., 1972, "The Anderson 'L' - An abnormally pressured gas reservoir in South Texas," J. Pet Tech. (Feb. 1972) p. 132-138.

Isokrari, O. F. and R. M. Knapp, 1976, "Natural gas production from geothermal geopressured aquifers," SPE6037, Society of Petroleum Engineers of AIME, 6200 North Central Expressway, Dallas, Texas 75206.

Knapp, R. M. and O. F. Isokrari, 1976, "Aspects of numerical simulation of future performance of geopressured geothermal reservoirs," Proceedings, Second Geopressured Geothermal Energy Conference, Center for Energy Studies, University of Texas at Austin, Austin, Texas (Feb. 23-25, 1976) vol. III.

APPENDIX

The basic equations for a deformable heterogeneous, anisotropic and nonisothermal reservoir as presented by Knapp and Isokrari (1976) are:

Momentum Transport in Water Phase:

$$\bar{\nabla} \cdot \frac{\rho_w K_{rw}}{\mu_w} K(\bar{\nabla}P_w - \frac{\rho_w}{144}\frac{\bar{g}}{g_c}\bar{\nabla}h) + \frac{\rho_{w_{sc}} q_w}{V_P^*} = (\phi S_w(\frac{\partial \rho_w}{\partial P})_T + (\rho_w S_w) \cdot (C_m + C_{rm}(1-\phi)))\frac{\partial P_w}{\partial t}$$

$$+ (\phi\rho_w)\frac{\partial Sw}{\partial t} + (\phi S_w(\frac{\partial Sw}{\partial T})_P)\frac{\partial T}{\partial t} \quad \ldots\ldots\ldots\ldots\ldots\ldots\ldots\ldots\ldots\ldots (1)$$

Momentum Transport in Gas Phase:

$$\bar{\nabla}(\rho_g \frac{K_{rg}}{\mu_g} K(\bar{\nabla}P_g - \frac{\rho_g}{144}\frac{\bar{g}}{\bar{g}_c}\bar{\nabla}h)) + \bar{\nabla}(\rho_w \frac{K_{rw}}{\mu_w} R_{sw} K(\bar{\nabla}Pw - \frac{\rho_w}{144}\frac{\bar{g}}{\bar{g}_c}\bar{\nabla}h)) + \frac{\rho_{w_{sc}} R_{w_{sc}} q_w}{V_P^*}$$

$$+ \frac{\rho_{g_{sc}} q_g}{V_P^*} = (\phi S_g(\frac{\partial \rho_g}{\partial P})_T + \phi S_w R_{sw}(\frac{\partial \rho_w}{\partial P}) + (\rho_w S_w R_{sw} + \rho_g S_g) \cdot (C_m + C_{rm}(1-\phi)))\frac{\partial P}{\partial t}$$

$$+ (\phi\rho_g)\frac{\partial S_g}{\partial t} + (\rho_w R_{sw}\phi)\frac{\partial S_w}{\partial t} + (\phi\rho_w S_w)\frac{\partial R_{sw}}{\partial t} + \phi((S_w R_{sw}(\frac{\partial \rho_w}{\partial T})_P$$

$$+ (1-S_w) \cdot (\frac{\partial \rho_g}{\partial T})_P))\frac{\partial T}{\partial t} \quad \ldots\ldots\ldots\ldots\ldots\ldots\ldots\ldots\ldots\ldots (2)$$

Energy Transport:

$$[(1-\phi)\rho_{rm}C_{vrm} + (S_g\rho_g C_{vg} + (1+R_{sw})\rho_w S_w C_{vw})\phi]\frac{\partial T}{\partial t} + [(\phi\rho_w S_w C_{vw}\bar{V}_w) + \phi(S_g\rho_g C_{vg}\bar{V}_g$$

$$+ S_w\rho_w R_{sw} C_{vw}\bar{V}_w)] \cdot \nabla T = \nabla \cdot [K_m] \cdot \nabla T + \frac{q_w C_{vw} T}{V_P^*}$$

$$+ \frac{q_g C_{vg} T}{V_P^*} + Q \quad \ldots\ldots\ldots\ldots\ldots\ldots\ldots\ldots\ldots\ldots (3)$$

Note that equations (1) to (3) assume that fluid is homogeneous.

$V_p^* = \Delta X_i \, \Delta Z_j \, W_i \, / \, 5.6146$ BBLS

C_m is the uniaxial compaction coefficient, psia $^{-1}$, defined as:

$$C_m = \frac{1 - \frac{\hat{K}}{\hat{K}_{rm}}}{K + \frac{4}{4}\hat{\mu}_P}$$

where:

$\hat{\mu}_P$ is the shear modulus of the porous rock

$\hat{K}(\hat{K}_{rm})$ is the bulk modulus of the porous rock (bulk modulus of the rock matrix)

$$S_w + S_g = 1 \quad \ldots\ldots\ldots\ldots\ldots\ldots\ldots\ldots\ldots\ldots\ldots\ldots\ldots\ldots (5)$$

$$P_g - P_w = P_c(S_w) \quad \ldots\ldots\ldots\ldots\ldots\ldots\ldots\ldots\ldots\ldots\ldots\ldots\ldots\ldots (6)$$

Constitutive Relationships:

1. Porosity - Pressure/temperature relationship for saturated rock:

$$\phi^{n+1} = \phi^n + (1-\phi^n)(C_{rm}+C_m)[\bar{P}^{n+1}-\bar{P}^n]\big|_T + (1-\phi^n)C_{Trm}[T^{n+1}-T^n]\big|_P \quad \ldots\ldots (7)$$

where:

$\bar{P}$ is of the wetting phase

2. Permeability - Pressure/temperature relationship for saturated rock

$$K^{n+1} = K^{n} \left[1.0 + \left(\frac{C_m + C_{rm}}{1 - \phi^{n}}\right)\left(\bar{P}^{n+1} - \bar{P}^{n}\right) + \left(\frac{C_{Trm}}{1-\phi^{n}}\right)\left(T^{n+1} - T^{n}\right)\right] \quad \ldots\ldots\ldots (8)$$

where:

$K^{n+1}(K^{n})$ = new value of permeability (old value of permeability)
Equation (8) can be shown to be equivalent to:

$$K^{n+1} = K^{n} \text{ EXP } \left[\frac{\phi^{n+1} - \phi^{n}}{(1-\phi^{n})(1-\phi^{n+1})}\right] \quad \ldots\ldots\ldots\ldots\ldots\ldots\ldots (9)$$

3. Compaction of a geologic medium due to fluid withdrawal

$$\Delta\bar{Z} = C_m \, \Delta\bar{P} L_Z + C_{TT} \, \Delta T L_Z \quad \ldots\ldots\ldots\ldots\ldots\ldots\ldots\ldots (10)$$

where:

$$C_{TT} = \frac{3 C_{Trm} \hat{K}}{\hat{K} + \frac{4}{3} \mu_P} \quad \ldots\ldots\ldots\ldots\ldots\ldots\ldots\ldots\ldots\ldots (11)$$

NOMENCLATURE

C_{rm}	Rock matrix compressibility, $psia^{-1}$
C_{Trm}	Coefficient of thermal expansion (T^{-1})
C_v	Specific heat of fluid, BTU/lb-^oF
g	Acceleration of gravity
gc	Acceleration constant (32.12 ft/sec/sec)
h	Depth below a reference datum, ft
K	Absolute permeability, tensor (.001127 x md)
K_r	Relative permeability, fraction
K_m	Thermal conductivity of saturated rock, BTU/D-ft-^oF
P	Pressure, psia
$\bar{P}$	Wetting phase pressure, psia
P_c	Capillary pressure, psia
q	Source - sink volumetric flow rate, STB/D
Q	Heat source strength, BTU/Day-ft^3
R_{sw}	Gas solubility in water (lbs/lbs)
S	Saturation, fraction
T	Temperature, ^oF
t	Time, days
$\bar{v}$	Macroscopic velocity, BBLS/D-ft^2
X,Z	X,Z direction, ft
W	Width (for vertical studies), thickness for horizontal studies

Greek

$\Delta X, \Delta Z$	Block dimensions
ρ	Phase density, lbm/ft^3
ϕ	Porosity
μ	Viscosity

Operators

$\nabla\cdot$	Divergence of a vector in fixed coordinate
$\bar{\nabla}\cdot$	Divergence of a vector in deforming coordinates

Subscripts

c	Constant
g	Gas
i	X direction node index
j	Z direction node index
rm	Rock matrix
w	Water

Superscripts

n	Old time level
n+1	New time level